Received: 10 March 2020 | Accepted: 24 March 2020

DOI: 10.1002/maco.202011657

ARTICLE

Materials and Corrosion

Investigation of the influence of iron-containing abrasives on the corrosion behaviour of the aluminium alloy AlSi1.2Mg0.4

Martin Babutzka | **Thoralf Müller** | **Jürgen Mietz** | **Andreas Burkert**

Division 7.6 Corrosion and Corrosion Protection, Bundesanstalt für Materialforschung und -prüfung (BAM), Berlin, Germany

Correspondence
Martin Babutzka, Division 7.6 Corrosion and Corrosion Protection, Bundesanstalt für Materialforschung und -prüfung (BAM), Unter den Eichen 87, 12205 Berlin, Germany.
Email: martin.babutzka@bam.de

Abstract

The corrosion resistance of aluminium surfaces is closely linked to the surface state after a grinding process. For years, iron-containing abrasive materials were suspected to lead to increased corrosion susceptibility after processing of aluminium surfaces. To prove a possible correlation between the iron content of an abrasive and the corrosion behaviour of aluminium components, scientific investigations and experimentally practical corrosion tests are necessary. For the current investigation, specimens of a technical Al-Si alloy from the same batch were used. The test specimens were mechanically ground with various resin-bonded model abrasives containing different iron contents. The performed corrosion tests did not reveal a negative influence of the different iron-containing abrasives on the corrosion behaviour of the Al–Si alloy. However, the most sensitive measuring method (electrochemical noise) showed differences in the surface activity depending on the type of abrasive.

KEYWORDS

aluminium, corrosion testing, grinding

1 | INTRODUCTION

Components made of aluminium alloys prove to be resistant against corrosion under atmospheric operating conditions. Aluminium is the second most important metallic material for automotive and mechanical engineering following steel.[1,2] Aluminium owes its high corrosion resistance to the ability to form a dense oxide layer (passive layer) on the material surface at neutral pH ranges. To increase the effectiveness of the corrosion protection, aluminium components are often coated with a conversion layer for temporary corrosion protection or anodised. The success and durability of a coating mainly depend on the surface state.[3] Contaminations at the metal surface can lead to undesired corrosion phenomena and subsequently to infiltration and delamination of the coating. As a result, high requirements regarding surface treatment are necessary. During aluminium treatment, grinding and blasting processes can lead to extraneous particles that stick to the workpiece surface. For years, industry representatives have expressed this assumption, especially in the case of iron-containing, synthetic resin-bonded abrasives for aluminium processing. It is presumed that iron particles from the grinding process could be incorporated into the aluminium surface leading to galvanic elements reducing the corrosion resistance of the surface locally. Until now, systematic, scientific investigations on the connection between the

iron content of an abrasive and corrosion behaviour are lacking.

The problem described above is known for blasted aluminium surfaces. The results of Klose and Kopp[4] for three differently blasted surfaces show that a surface treated with CrNi steel blasting grain is most susceptible to corrosion, which they traced back to incorporated iron particles. They mention that only blasting abrasives are approved for blasting processes which do not contain iron contaminations. However, an in-depth analysis with respect to possible correlations or explanation attempts was not given.

Furthermore, the correlation between the number of intermetallic phases in the form of Al(Fe, Si, Mn) segregates and the corrosion resistance of Al–Fe alloys has been described in the literature. Increased content of such precipitations within the material led to a significant loss of the corrosion resistance.[5] Seri and Furumata[6] have proven that increased iron content in the precipitations favours the initiation of pitting. Whether analogies regarding the phenomena caused by iron particles impressed during the grinding process exist has not been proven yet.

Industrial companies are hence interested in different questions that require clarification. For a manufacturer of abrasives, it is technically very complex to guarantee completely iron-free abrasives. The influence of the iron content of abrasives on the corrosion behaviour of aluminium alloys is investigated by means of conventional corrosion tests and electrochemical corrosion investigations in this paper as the first approach to the presented issues.

2 | EXPERIMENTAL

2.1 | Material and specimen preparation

The technical aluminium alloy EN AW-6016 (EN AW-AlSi1.2Mg0.4) designated for the investigations was provided by Hydro Aluminium Rolled Products GmbH, Bonn. The alloy was delivered as sheets manufactured from one batch ensuring uniform alloying elements for all test specimens. The composition of the alloy was determined by atomic emission spectroscopy (Table 1).

All alloying contents comply with the limits defined in the standard DIN EN 573-3.[7] It has to be noted that the technical aluminium and aluminium alloys already contain a certain amount of iron, which has to be considered in the following corrosion tests. The present alloy exhibited an iron content of 0.2 wt%, which is below the threshold value of 0.5 wt% according to the standard DIN EN 573-3.

The aluminium alloy sheets were cut into separate specimens with dimensions of $50 \times 100 \times 1$ mm. Specimens were provided with a drill hole (diameter of 9 mm at the edge of a specimen) for adjustment. The specimens were cleaned from coarse contaminants resulting from processing with petroleum ether and degreased ultrasonically by means of acetone and ethanol. To achieve an iron-free surface condition before the grinding with iron-containing abrasives, the specimens were pickled for 5 min after cutting and cleaning. As pickling solution, nitric acid (HNO_3; $\rho = 1.42$ g/ml) was used to remove extraneous deposits and larger corrosion products from the surface while ensuring a negligible reaction of the base metal at room temperature. The pickling treatment was conducted according to DIN EN ISO 8407.[8]

2.2 | Metallographical investigations of the as-received material

The aim of the metallographic investigations of the as-received material was to guarantee a homogeneous microstructure condition permitting high comparability of the different specimens manufactured from the as-received material. Metallographic cross sections (flat and longitudinal section) enabled characterisation of the microstructure of the as-received material and documentation of precipitations within the aluminium matrix. A representative test sheet was embedded, polished, etched and, subsequently, investigated by a light optical microscope with ×200 magnification. Hydrofluoric acid (HF; 5%) with molybdic acid was used as the etching agent. Microscopy images of flat and longitudinal sections were prepared and assessed with respect to the type of precipitations, size of precipitations and microstructure condition.

TABLE 1 Chemical composition of the aluminium alloy EN AW-6016 according to DIN EN 573-3[7] and values measured with atomic emission spectroscopy (AES), in wt%

	Si	Fe	Cu	Mn	Mg	Cr	Zn	Ti	Al
Range according to DIN EN 573-3	1.0–1.5	≤0.50	≤0.20	≤0.20	0.25-0.6	≤0.100	≤0.200	≤0.15	balance
AES	1.28	0.20	0.01	0.06	0.29	0.001	0.006	0.02	balance

2.3 | Preparation of the test surfaces by means of mechanical grinding

The preparation of the test surfaces of the specimens was performed by a defined grinding process. As abrasives, resin-bonded grinding wheels (special model abrasives provided by Hermes Schleifmittel & Co. KG) with a significant variation of the iron content were used. The abrasives further differed regarding the type of contained iron. Table 2 gives an overview of the model abrasives used and their special features. Abrasive C was an iron-reduced type, whereas Abrasives A and B possessed a high iron content. Abrasive A contained mainly iron oxide and Abrasive B was produced by the addition of pure iron in the form of iron powder.

The grinding process was conducted by means of a random rotary sander (Festool GmbH provided by Starcke GmbH & Co. KG). An integrated dust extraction prevented the formation and deposition of aluminium grinding dust. Twelve specimens were simultaneously, mechanically ground with each model abrasive. The specimens were mechanically ground with the random rotary sander three times vertically to the rolling direction and three times along the rolling direction of the sheets. The total grinding time was 2 min for each case. Each grinding wheel was used only once. The random rotary sander was cleaned after each grinding process and after the replacement of the grinding wheel. To guarantee a defined and comparable grinding pressure for all grinding processes, a weight of 3 kg was put on the grinding head of the random rotary sander. After grinding, the specimens were cleaned by acetone and ethanol to remove the remaining grinding dust from the specimen surface.

2.4 | Surface morphology characterisation and identification of possible iron residues after the grinding process

The surface morphology of the mechanically ground specimens was assessed by means of a true colour confocal microscope Axio CSM 700 (Zeiss). The confocal microscope utilises a light optical system with a confocal beam path enabling scanning of the specimen surface in x-, y-, and z-directions and achieving an unlimited depth of field. Images of the surface with ×10 magnification were prepared from the as-received state as well as from the mechanically ground surfaces. The averaged peak-to-valley height (*Rz*), the arithmetic averaged roughness value (*Ra*) and the quadratic averaged roughness value (*Rq*) according to DIN EN ISO 25178[9] were determined as characteristic parameters of the surface. As the mechanically ground surfaces were aperiodic profiles, the determined roughness values are not according to standard and can be erroneous but they served as a rough estimate of the surface profile. After the conventional corrosion tests, the mechanically ground surfaces were scanned by means of a confocal microscope and scanned for iron residues in the form of red rust spots.

2.5 | Corrosion investigations

2.5.1 | Salt spray test

The mechanically ground aluminium alloy test sheets were exposed in a salt spray chamber (SKBW 1000 A-SC; Liebisch Labortechnik) according to DIN EN ISO 9227.[10] The aluminium alloy specimens were arranged with a tilt angle of 45° in the chamber whereby the mechanically ground surface faced upwards. Two specimens per abrasive were arranged horizontally and one specimen per abrasive vertically (see Figure 1). The test was performed at a constant chamber temperature of 35°C under permanent spraying with a chloride-containing fog using a 5% sodium chloride solution. The test sheets were removed from the chamber and dried in air after 24-hr test duration. Subsequently, the mechanically ground surfaces were photographed with high-resolution and visually assessed.

2.5.2 | Condensed water test without chloride contamination

To investigate the corrosion behaviour under permanently humid conditions, three specimens per abrasive were

TABLE 2 Model abrasives for the preparation of the surface states by mechanical grinding

	Special feature	Analytical Fe-content (data provided by Hermes Schleifmittel & Co. KG)
Abrasive A	Addition of iron oxide (chemically bound iron)	8,430 ppm
Abrasive B	Addition of iron from iron powder (chemically unbound iron)	11,600 ppm
Abrasive C	Low iron abrasive	67 ppm

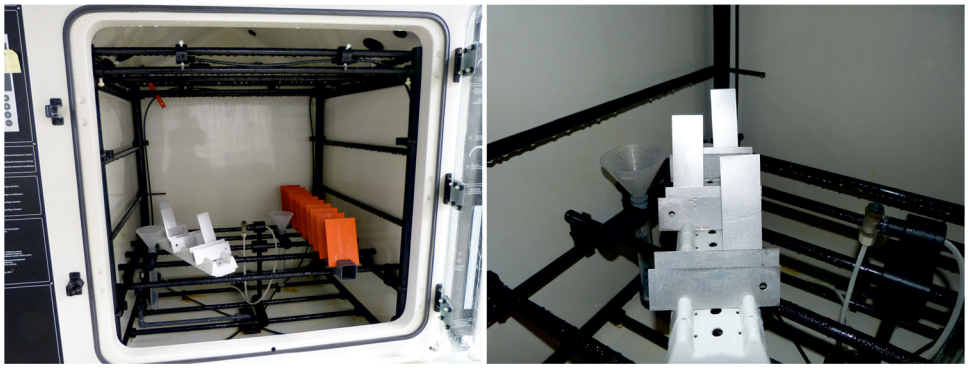

FIGURE 1 Specimen arrangement of the mechanically ground AlSi1.2Mg0.4 sheets within the salt spray chamber [Color figure can be viewed at wileyonlinelibrary.com]

subjected to a condensed water climate test in a climate chamber (Constanzo KB 300; Liebisch Labortechnik) according to DIN EN ISO 6270.[11,12] The test was carried out with a constant moistening of 100% relative humidity (r. h.) and a chamber temperature of 40°C without the addition of chlorides. The specimens were arranged hanging vertically in the test chamber to avoid stagnating water. The specimens were removed from the chamber after a test duration of 48 hr and dried in air. Subsequently, the mechanically ground surfaces were photographed with high-resolution and visually assessed.

2.5.3 | Combined test with addition of a chloride load

The combined test included the combination of a one-time chloride loading of the specimen surface followed by exposure to a constant climate. The aim of the combined test was the laboratory simulation of specimen exposure under a marine atmosphere with a chloride deposition and concentration on the specimen surfaces typical for this type of atmosphere. One representative specimen of each abrasive was selected and a 5% sodium chloride solution was sprayed across its entire surface. Subsequently, the test sheets with chloride load were exposed in a climate chamber (HC 2057; Vötsch Industrietechnik GmbH) at a constant humidity of 80% r. h. and a temperature of 30°C. The specimens were arranged with a tilt angle of 45° in the chamber whereby the mechanically ground surface faced upwards. The specimens were removed from the chamber after a test duration of 18 days and dried in air. Subsequently, the mechanically ground surfaces were photographed with high-resolution and visually assessed.

2.5.4 | Long-term exposure under atmospheric conditions

Free weathering tests were conducted at exposure sites in an urban atmosphere in the city of Berlin and in the marine atmosphere on the Island of Heligoland (Figure 2)

FIGURE 2 Exposed AlSi1.2Mg0.4 sheets on the roof of the BAM main building in the city of Berlin (left, urban atmosphere) and on the island of Heligoland (right, marine atmosphere) [Color figure can be viewed at wileyonlinelibrary.com]

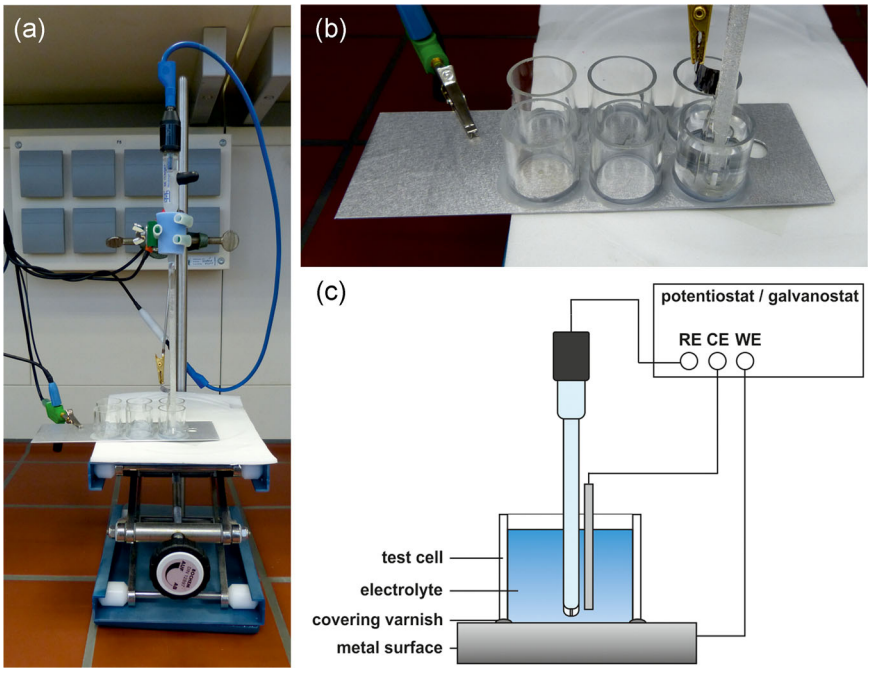

FIGURE 3 Measuring set-up for the electrochemical corrosion investigations at AlSi1.2Mg0.4: (a) overview, (b) test sheet with test cells and three-electrode arrangement, (c) schematic sketch [Color figure can be viewed at wileyonlinelibrary.com]

following DIN EN ISO 8565.[13] Three specimens per abrasive were installed with a tilt angle of 45° on the test racks. The specimens were directly exposed to the atmosphere and, hence, also to precipitation. On the Island of Heligoland, three additional specimens per abrasive were exposed under sheltered conditions and thus protected against precipitation. Rinsing of chlorides was prevented and the accumulation of air constituents on the specimen surface was accelerated by sheltering. The specimens were installed with a tilt angle of 90°. The test specimens were exposed beginning from September 14, 2015 (Berlin) and September 15, 2015 (Island of Heligoland) and removed from the exposure racks after 270 days of weathering. The mechanically ground surfaces were photographed and visually assessed. The following corrosivity categories regarding pure aluminium were determined for the different atmospheres of long-term exposure:

(a) outdoor weathering in an urban atmosphere in the city of Berlin: C2,
(b) outdoor weathering in the marine atmosphere on the Island of Heligoland: C2,
(c) sheltered weathering in the marine atmosphere on the Island of Heligoland: C3.

2.5.5 | Electrochemical corrosion measurements

The electrochemical measurements of the mechanically ground surfaces were carried out under laboratory conditions at room temperature (23 ± 2°C). The investigations were performed with small test cells made of acrylic glass that were attached to the surface. The measuring cells were covered with varnish at the contact points to the substrate

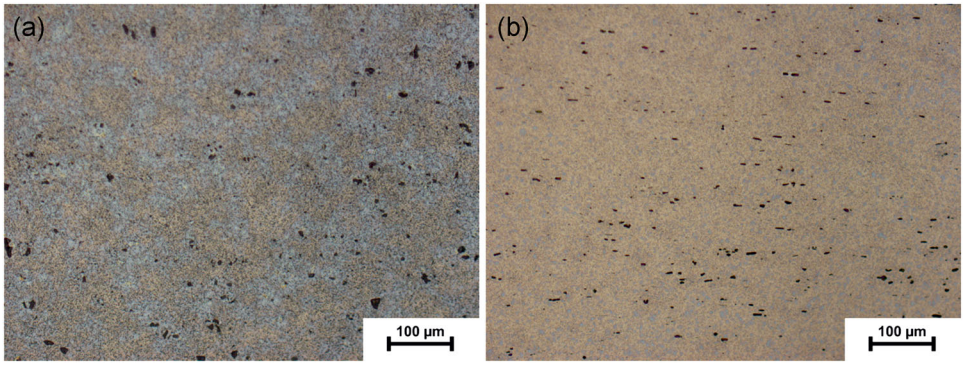

FIGURE 4 Microstructure of alloy AlSi1.2Mg0.4, optical microscopy, ×200 magnification, 5% HF with molybdic acid. (a) flat section and (b) longitudinal section [Color figure can be viewed at wileyonlinelibrary.com]

(specimen surface) to prevent crevice effects. The measuring cell arrangement enabled multiple electrochemical measurements on the specimen surface. The effective measuring area was 3.14 cm^2. A three-electrode-arrangement was used for the investigations. A saturated silver/silver chloride electrode (Ag/AgCl; $E_{NHE} = +199$ mV) and a platinum sheet were used as the reference electrode (RE) and counter electrode (CE), respectively. The specimen was the working electrode (WE). Figure 3 shows the measuring set-up and a schematic sketch of the measuring principle. Prior to the measurements, the mechanically ground specimens were equipped with six test cells each and stored at laboratory atmosphere (approx. 30% r. h.) for 2 hr. Subsequently, critical potential values were determined by means of dynamic polarisation at three measuring points and electrochemical noise measurements were conducted at the other three measuring points. For all electrochemical measurements, a 0.01 M sodium chloride solution with a pH-value of 6 (unbuffered) was used.

Potentiodynamic polarisation to determine critical potential values

At the beginning of the measurements, the test cell was filled with the test electrolyte. As evaluation parameter, the open circuit potential (E_{OCP}) was determined after 600 seconds of contact to the electrolyte. Subsequently, the specimen was polarised potentiodynamically in the anodic direction starting from a potential −150 mV relative to the open circuit potential. The potential scan rate dE/dt was 0.5 mV/s. The first potential value after exceeding a threshold current density of 10 μA/cm^2 was defined as the critical pitting potential. The measurements were carried out with a potentiostat/galvanostat Reference 600 (Gamry Instruments). The mean values and deviations of open circuit potential and the pitting potentials, respectively, were calculated from three measurements at each surface state. All potentials in the results section refer to the Ag/AgCl reference electrode unless stated otherwise.

Electrochemical noise measurements

At the beginning of the measurements, the test cell was filled with the test electrolyte and the open circuit potential was recorded for 600 seconds without external polarisation. Subsequently, the specimen was polarised with a constant undercritical test potential of −550 $mV_{Ag/AgCl}$ for 20 min whereby the current and the current noise were measured and analysed afterwards. An undercritical test potential was chosen in consideration of the critical pitting potentials determined by potentiodynamic polarisation. The measuring range for the current and current noise was 100 μA, whereby the current noise was amplified by a factor of 100. The sampling rate was 100 Hz. The measurements were

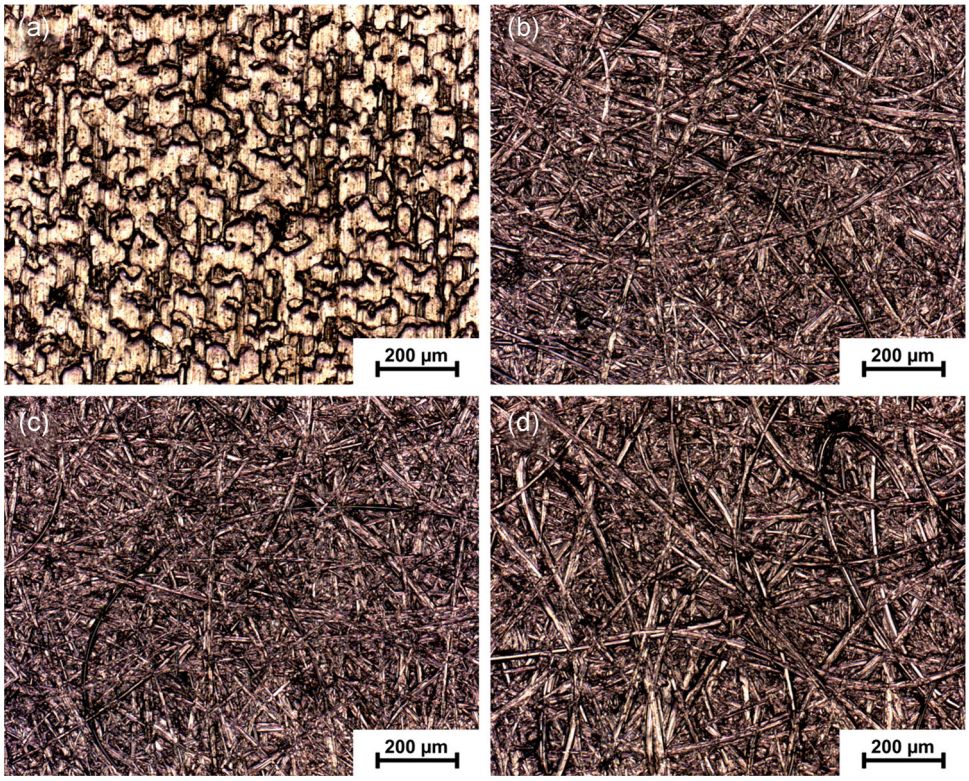

FIGURE 5 Surface morphology of the alloy AlSi1.2Mg0.4 by means of confocal microscopy, ×10 magnification. (a) as-received, (b) mechanically ground with Abrasive A, (c) mechanically ground with Abrasive B, and (d) mechanically ground with Abrasive C [Color figure can be viewed at wileyonlinelibrary.com]

TABLE 3 Determined roughness parameters according to DIN EN ISO 25178 for AlSi1.2Mg0.4 mechanically ground with different abrasives, mean values and standard deviation

	Initial state (rolled surface)	Abrasive A	Abrasive B	Abrasive C
Rz (μm)	7.2 ± 1.9	7.3 ± 0.5	11.7 ± 1.9	15.8 ± 2.8
Ra (μm)	1.0 ± 0.1	1.0 ± 0.1	1.3 ± 0.1	1.4 ± 0.2
Rq (μm)	1.2 ± 0.1	1.3 ± 0.1	1.8 ± 0.2	2.2 ± 0.5

performed in a Faraday cage to avoid influences due to external or stray currents. The potentiostat used was a potentiostat–galvanostat IMP-88-PC-R (Jaissle). The current density averaged over the test duration of 20 min and the standard deviation of the current noise were determined as characteristic values from three measurements of each surface state.

3 | RESULTS AND DISCUSSION

3.1 | Metallographic investigation of the as-received material

Metallographic cross-sections of the as-received material did not indicate any unusual anomalies of the microstructure. Figure 4 presents micrographs of flat and longitudinal sections obtained with 5% HF with molybdic acid. All the optical microscopy images revealed a homogeneous microstructure consisting of the aluminium matrix and finely dispersed Al–Si–Mg segregations (black areas) with a typical size. No line-shaped segregations were observed in the flat section as well as in the longitudinal section. Furthermore, no unusual segregations or inhomogeneities were found in the microstructure. Thus, the delivered alloy represented a suitable and typical initial state for the intended investigations.

3.2 | Characterisation of surface morphology and identification of possible iron residues after the grinding process

The grinding process generated different surface states and profiles depending on the abrasive used. Figure 5 shows the corresponding aluminium alloy surfaces documented by means of confocal microscopy. The mechanically ground surfaces revealed a similar grinding pattern for all abrasives tested. Surfaces with undirected grinding marks were generated on all specimens by means of the random rotary sander. The surface mechanically ground with Abrasive C appeared a little bit rougher than the other surfaces and possessed deeper grinding marks. On all mechanically ground surfaces, confocal microscopy did not reveal coarse contaminations and residues. The determined roughness parameters confirmed the impression of the optical assessment of the surface morphology. Table 3 summarises the mean values and the standard deviations of the different roughness parameters. Differences in the surface roughness parameters were detected despite comparable grinding patterns. Significant differences were detected especially for *Rz*. Abrasive A revealed the lowest roughness. *Rz* for Abrasive C was nearly twice as high. For a reliable assessment, however, the high standard deviations due to the aperiodic profile have to be considered.

3.3 | Conventional corrosion tests

3.3.1 | Salt spray test

The salt spray test should verify whether red rust spots due to iron residues can be found after grinding with the different abrasives. After 24 hr of salt spray exposure, all mechanically ground test specimens showed the same appearance of the surface independent of the abrasive used (Figure 6). Depending on the orientation within the salt spray chamber, dark discolorations, and run-off

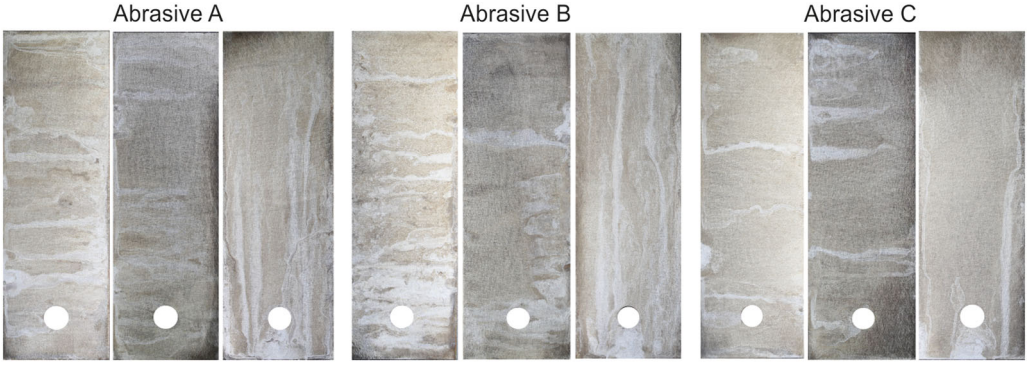

FIGURE 6 Appearance of the surfaces of AlSi1.2Mg0.4 mechanically ground with different iron-containing abrasives after a 24-hr salt spray testing [Color figure can be viewed at wileyonlinelibrary.com]

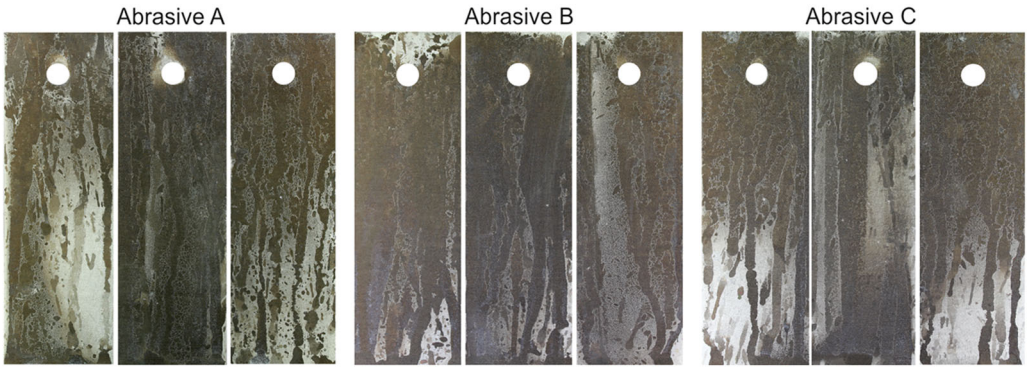

FIGURE 7 Appearance of the surfaces of AlSi1.2Mg0.4 mechanically ground with different iron-containing abrasives after a 48-hr condensed water test [Color figure can be viewed at wileyonlinelibrary.com]

traces caused by contact with moisture were seen on all test surfaces. No signs of red rust were observed on the mechanically ground surfaces. Discolourations on the surface resulted from layer formation processes due to the permanently humid atmosphere and the increased temperature. They were not caused by iron deposits or iron corrosion products despite their brownish-black colour.

3.3.2 | Condensed water test without chloride contamination

The appearance of the mechanically ground aluminium alloy specimens after 48 hr of chloride-free condensed water test is shown in Figure 7. No signs of red rust were observed on the aluminium alloy specimens analogous to the results of the salt spray test. No influence of the iron content and type of added iron from the different abrasives was identified. Independent of the used abrasive, all specimens revealed dark discolourations and run-off traces of water on the surface. As the specimens were arranged vertically in the chamber, the mechanically ground test side as well as the nonground as-received back side revealed the described dark discolourations. These discolourations were not caused by iron residues or corrosion reactions of iron but by oxide layer formation processes, which were accelerated by contact with moisture and elevated temperature. This phenomenon is known for aluminium and aluminium–zinc coatings and is described in the literature as wet storage stain or black rust stain.[14-16] The formed oxide layers are dense, tightly adhering and cannot be removed by a subsequent pickling process with HNO_3. To illustrate this, Figure 8 shows a specimen mechanically ground with Abrasive C after 48 hr condensed water test and after pickling with HNO_3 for 10 min.

FIGURE 8 Appearance of the surfaces of AlSi1.2Mg0.4 mechanically ground with Abrasive C: (a) after 48-hr condensed water test, (b) after 48-hr condensed water test and subsequent pickling with nitric acid for 10 min [Color figure can be viewed at wileyonlinelibrary.com]

3.3.3 | Combined test with addition of a chloride load

The combined test was conducted to simulate exposure with chloride deposits on the surface. The appearance of the mechanically ground specimens after 18 days combined test is summarised in Figure 9. The surfaces exhibited whitish-crystalline deposits representing a dried salt film. At locations with permanent wet conditions due to local chloride concentrations, dark discolourations as a result of layer formation processes were observed analogous to the results of the salt spray test. None of the mechanically ground surfaces revealed signs of aluminium corrosion (e.g., pitting) or red rust from iron

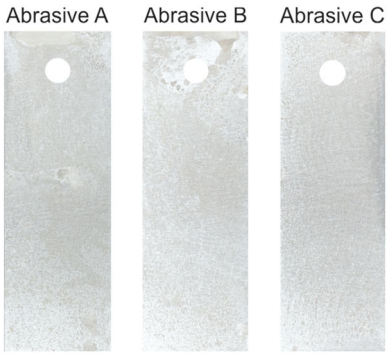

FIGURE 9 Appearance of the surfaces of AlSi1.2Mg0.4 mechanically ground with different iron-containing abrasives after 18 days of combined test with chloride load [Color figure can be viewed at wileyonlinelibrary.com]

residues. Thus, no influence of the iron content and type of iron added to the abrasive could be proven.

3.3.4 | Long-term exposure under atmospheric conditions

The mechanically ground specimens were exposed to different atmospheric conditions in addition to conventional chamber tests. The appearances of the mechanically ground specimens after 270 days of long-term exposure to the urban atmosphere in the city of Berlin and to the marine atmosphere on the Island of Heligoland are shown in Figure 10. After 270 days of long-term exposure, no signs of red rust were observed on the mechanically ground aluminium alloy surfaces for all types of abrasives. All specimens revealed local corrosion on the surface. No differences regarding the abrasive used for grinding were determined. Hence, no influence of the iron content and the type of iron added to the abrasives could be found.

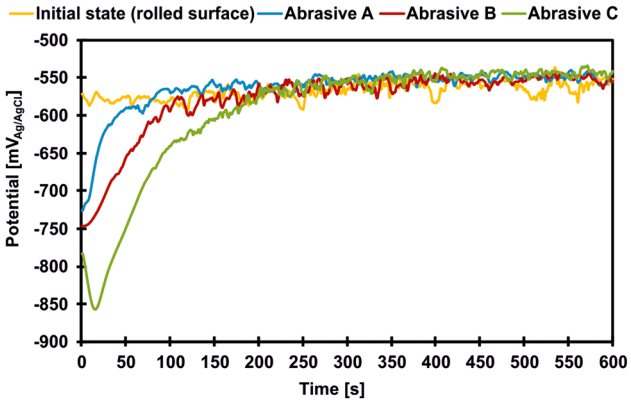

FIGURE 11 Potential versus time curves of mechanically ground surfaces of AlSi1.2Mg0.4 in 0.01 M NaCl solution (pH = 6, unbuffered) [Color figure can be viewed at wileyonlinelibrary.com]

3.4 | Electrochemical corrosion investigations

3.4.1 | Open circuit potential

Figure 11 shows the open circuit potential versus time curves for the different mechanically ground surfaces in contact with a 0.01 M NaCl solution over a period of 600 s. At the beginning of the measurement, the open circuit potentials of the mechanically ground specimens revealed very negative potentials between −720 and −780 $mV_{Ag/AgCl}$ indicating an active state of the specimen surface after the grinding treatment. Subsequently, the open circuit potentials of all mechanically ground specimens significantly increased within 150 s due to ongoing passivation in the electrolyte and stabilised at about −550 $mV_{Ag/AgCl}$. The non-ground as-received state revealed a higher potential level from the beginning. This potential level was within the passive potential range of

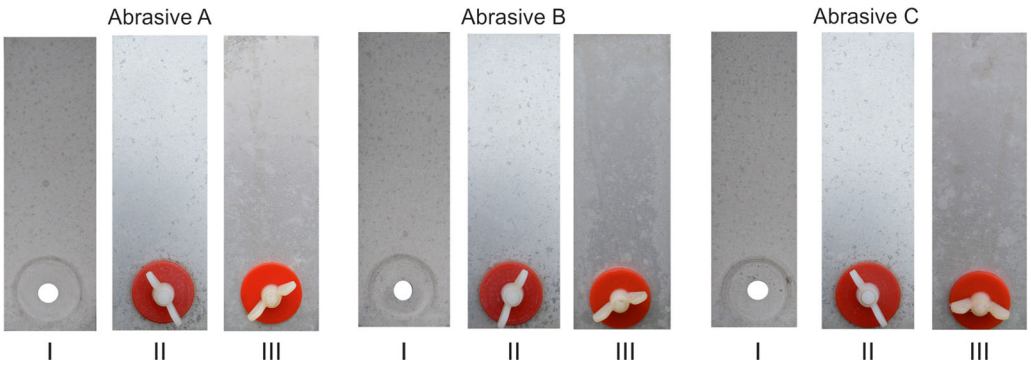

FIGURE 10 Appearance of the surfaces of AlSi1.2Mg0.4 mechanically ground with different iron-containing abrasives after 270 days of outdoor exposure: I...outdoor weathering in an urban atmosphere in the city of Berlin (C2 atmosphere), II...outdoor weathering in the marine atmosphere on the Island of Heligoland (C2 atmosphere), III...sheltered weathering in the marine atmosphere on the Island of Heligoland (C3 atmosphere) [Color figure can be viewed at wileyonlinelibrary.com]

TABLE 4 Open circuit potentials (E_{OCP}) of mechanically ground and as-received surfaces of AlSi1.2Mg0.4 after 600 seconds contact with 0.01 M NaCl solution (pH = 6, unbuffered), mean values and standard deviations

	Initial state (rolled surface)	Abrasive A	Abrasive B	Abrasive C
E_{OCP}	-548 ± 52 $mV_{Ag/AgCl}$	-605 ± 56 $mV_{Ag/AgCl}$	-590 ± 74 $mV_{Ag/AgCl}$	-605 ± 7 $mV_{Ag/AgCl}$

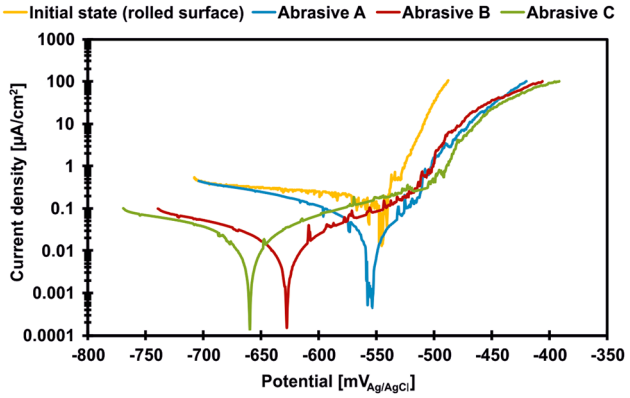

FIGURE 12 Current density-potential curves from potentiodynamic polarisation of mechanically ground surfaces of AlSi1.2Mg0.4 in 0.01 M NaCl solution (pH = 6, unbuffered) [Color figure can be viewed at wileyonlinelibrary.com]

aluminium. However, small potential fluctuations could be seen caused by surface activities and furthermore by the chloride content of the used test electrolyte. Table 4 represents the open circuit potentials after 600 seconds contact with the electrolyte. As all mean values and standard deviations of the open circuit potential were within a comparable potential range, the significance of the iron content and the type of iron in the abrasive on the passivation behaviour could not be verified.

3.4.2 | Determination of critical potential values by means of potentiodynamic polarisation

The determination of pitting potentials was performed by current density-potential curves obtained by potentiodynamic polarisation of the tested surface states (Figure 12). The three mechanically ground surface versions indicated similar current density-potential curves. The free corrosion potentials differed from each other. However, similar pitting potentials were observed following the passive range of the curves. The as-received state showed a slightly worse pitting potential compared to the mechanically ground specimens. Table 5 summarises the pitting potentials determined at a threshold current density of 10 $\mu A/cm^2$. All mechanically ground surfaces had nearly identical mean values. Due to overlapping deviation ranges, an equal pitting potential can be assumed. Thus, for the tested surfaces, a significant influence of the different abrasives on the pitting corrosion behaviour could not be proven.

3.4.3 | Electrochemical noise measurements

The electrochemical noise measurements were performed at a constant test potential of -550 $mV_{Ag/AgCl}$ in the subcritical potential range below the pitting potential. The recorded current density and current noise are shown exemplarily in Figure 13 for a selected measurement per abrasive. The surfaces mechanically ground with Abrasive B revealed the highest surface activity clearly indicated by the increased current noise and the increase of the current density in the current curve. The surface mechanically ground with Abrasive C did not show a significant current increase during the whole measuring period and the current noise also indicated only small noise transients. The initial state behaved similar to the surface mechanically ground with Abrasive C. Figure 14 summarises the characteristic values determined from the electrochemical noise measurements for all tested surface variants. The summarised results clarify that the respective abrasive variants can lead to differences in the surface activity of the specimens for the given test conditions. It is notable that the increased iron content from the addition of iron powder to Abrasive B can lead to an increased surface activity of the aluminium alloy. However, this correlation did not apply to the entire mechanically ground surface, but to individual measuring points indicated by the wide range of the standard deviation. Nevertheless, the surfaces

TABLE 5 Pitting potentials (E_{pit}) of mechanically ground and as-received surfaces of AlSi1.2Mg0.4 in contact with 0.01 M NaCl solution (pH = 6, unbuffered), determined by potentiodynamic polarisation, mean values and standard deviations

	Initial state (rolled surface)	Abrasive A	Abrasive B	Abrasive C
E_{pit}	-510 ± 10 $mV_{Ag/AgCl}$	-481 ± 9 $mV_{Ag/AgCl}$	-485 ± 16 $mV_{Ag/AgCl}$	-481 ± 1 $mV_{Ag/AgCl}$

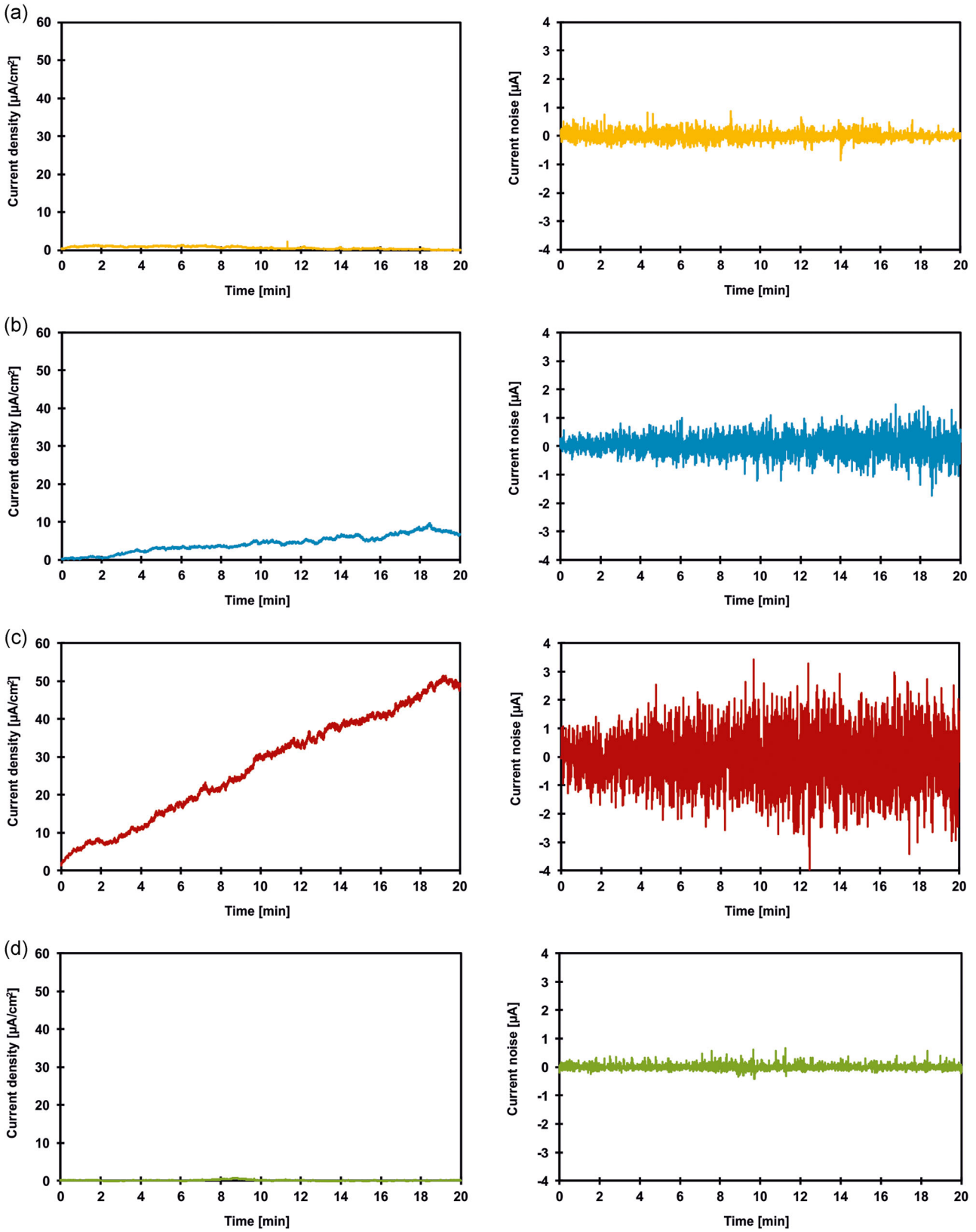

FIGURE 13 Selected results of the electrochemical noise measurements at mechanically ground surfaces of AlSi1.2Mg0.4 at a constant potential of $-550\ mV_{Ag/AgCl}$, 0.01 M NaCl solution (pH = 6, unbuffered). (a) Initial state (rolled surface): little surface activity, (b) Abrasive A: low surface activity, (c) Abrasive B: high surface activity, and (d) Abrasive C: little surface activity [Color figure can be viewed at wileyonlinelibrary.com]

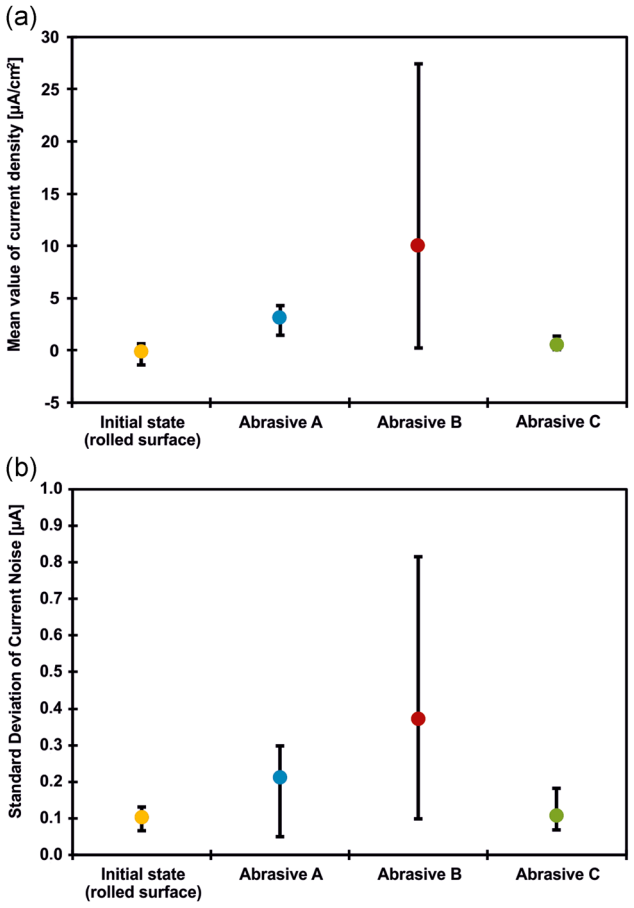

FIGURE 14 Analysis of electrochemical noise measurements of mechanically ground and as-received surfaces of AlSi1.2Mg0.4 at a constant potential of $-550\ mV_{Ag/AgCl}$, 0.01 M NaCl solution (pH = 6, unbuffered). (a) Analysis of the current density averaged over the whole test duration and (b) analysis of the standard deviation of the current noise [Color figure can be viewed at wileyonlinelibrary.com]

mechanically ground with Abrasive B differed significantly from the other surfaces.

4 | SUMMARY AND CONCLUSIONS

By means of a defined grinding process, different surface states were generated at test sheets of the aluminium alloy AlSi1.2Mg0.4, which were subsequently subjected to various corrosion tests. In particular, the iron content and the type of added iron of the provided abrasives were varied to prove possible differences in the corrosion behaviour of mechanically ground surfaces due to iron particle residues on the surface of the aluminium alloy.

The grinding process led to comparable surface morphologies and grinding patterns of all mechanically ground surfaces but with differences in the surface roughness. Significant differences were observed for the arithmetic mean roughness value *Rz*: Grinding with Abrasive C (low iron abrasive) revealed the highest roughness. The differences in surface roughness did not provide a measurable influence on the corrosion resistance of the surfaces as proven by different corrosion tests. Embedded iron particles or significant iron contaminations resulting from the grinding process could not be detected microscopically for any of the specimens.

The influence of the iron content or the type of added iron to the abrasives on the corrosion behaviour of the aluminium alloy could not be identified by conventional corrosion tests. None of the investigated specimens revealed red rust formation. Increased corrosion of the aluminium alloy was not measurable with increased iron content of the abrasive. The specimens showed discolourations and run-off stains from water on the mechanically ground as well as on the as-received surfaces after the chamber tests. These discolourations, as for example shown in Figure 7, can possibly be mixed up with iron corrosion products due to their brownish-black colour. But in fact, they are relatively thick, strongly adhering aluminium oxide layers forming at permanently humid conditions and elevated temperatures occurring in test chambers. This phenomenon is described as wet storage stain or black rust stain in the literature and is not relevant under typical atmospheric corrosion conditions.

Practically relevant test results with respect to the atmospheric corrosion resistance of mechanically ground specimens can only be provided by exposure tests at real atmospheres as they avoid the intensification of test conditions (e.g., temperature, humidity). After 270 days of exposure in the urban and marine atmosphere, no differences of the corrosion behaviour were observed for surfaces mechanically ground with different iron-containing abrasives.

The electrochemical investigations did not reveal a dependence of the corrosion behaviour on the type of iron-containing abrasive in most cases. The open circuit and the pitting potentials did not indicate an influence on the corrosion behaviour due to the different abrasives. All mechanically ground surfaces exhibited a similar corrosion and passivation behaviour during the electrochemical tests independent of the type of abrasive. Differences in the surface activity of the mechanically ground specimens were detected only by using highly sensitive electrochemical noise measurements. These differences cannot be clearly traced back to iron particles and residues incorporated in the specimen surface as such particles could not be verified optically by means of confocal microscopy. However, it should be noted that Abrasives A and B have different binding states (Abrasive A: chemically bound iron from iron oxide, Abrasive B:

chemically unbound iron from iron powder) which can also lead to possible differences of the surface activity due to the altered grinding behaviour of the abrasives. The differences in the surface activity did not seem to result in measurable differences in the practical corrosion behaviour of the mechanically ground surfaces with regard to the performed outdoor exposure tests.

The negative influence of different iron-containing abrasives on the corrosion behaviour of the aluminium alloy AlSi1.2Mg0.4 could not be determined by means of different corrosion tests. Highly sensitive electrochemical noise measurements showed that grinding with different iron-containing abrasives can result in different surface activities.

ACKNOWLEDGEMENT

The authors acknowledge the financial support of the FGS—Forschungsgemeinschaft Schleiftechnik e.V. and the member companies of the Technical Committee for the supply of the special abrasives and grinding devices.

ORCID

Martin Babutzka http://orcid.org/0000-0002-3074-2203
Jürgen Mietz http://orcid.org/0000-0002-2878-7576

REFERENCES

[1] D. Wieser, in *Tagungsband zur GfKORR-Jahrestagung 2011, Aluminium—bereit für die Zukunft*, (Hrsg.: GfKORR—Gesellschaft für Korrosionsschutz e.V.), GfKORR, Frankfurt am Main, **2011**, p. 5–12.
[2] M. C. Reboul, B. Baroux, *Mater. Corros.* **2011**, *62*, 215.
[3] M. Walter, in *Tagungsband zur GfKORR-Jahrestagung 2011, Aluminium—bereit für die Zukunft*, (Hrsg.: GfKORR—Gesellschaft für Korrosionsschutz e.V.), GfKORR, Frankfurt am Main, **2011**, p. 67–73.
[4] S. G. Klose, J. Kopp, *Tagungsband zur GfKORR-Jahrestagung 2011, Aluminium—bereit für die Zukunft*, (Hrsg.: GfKORR—Gesellschaft für Korrosionsschutz e.V.), GfKORR, Frankfurt am Main, **2011**, p. 36–55.
[5] Korrosion und Korrosionsschutz, Band 2: Korrosion der verschiedenen (Hrsg.: W. E. Kunze), WILEY-VCH Verlag GmbH, Weinheim, **2001**.
[6] O. Seri, K. Furumata, *Mater. Corros.* **2002**, *53*, 111.
[7] EN 573-3:2019, Aluminium and aluminium alloys—Chemical composition and form of wrought products—Part 3: Chemical composition and form of products.
[8] EN ISO 8407,2014, Corrosion of metals and alloys—Removal of corrosion products from corrosion test specimens (ISO 8407:2009).
[9] EN ISO 25178-2:2012, Geometrical product specifications (GPS)—Surface texture: Areal—Part 2: Terms, definitions and surface texture parameters (ISO 25178-2:2012).
[10] EN ISO 9227:2017, Corrosion tests in artificial atmospheres—Salt spray tests (ISO 9227:2017).
[11] EN ISO 6270-1:2018, Paints and varnishes—Determination of resistance to humidity—Part 1: Condensation (single-sided exposure) (ISO 6270-1:2017).
[12] EN ISO 6270-2:2018, Paints and varnishes—Determination of resistance to humidity—Part 2: Condensation (in-cabinet exposure with heated water reservoir) (ISO 6270-2:2017).
[13] EN ISO 8565:2011, Metals and alloys—Atmospheric corrosion testing—General requirements (ISO 8565:2011).
[14] I. O. Wallinder, W. He, P. E. Augustsson, C. Leygraf, *Corros. Sci.* **1999**, *41*, 2229.
[15] Verein zur Hebung der Information über Aluminiumfenster und –fassaden, (Hrsg.: Aluminium-Fenster-Institut), *Qualitätshandbuch für Fenster und Fassaden aus Aluminium*, Teil 2 Werkstoff, 1. Auflage, Wien **1997**.
[16] Merkblatt 121 Korrosionsschutzsysteme für Bauelemente aus Stahlblech, 1 (Hrsg.: Stahl-Informations-Zentrum), *Merkblatt 121 Korrosionsschutzsysteme für Bauelemente aus Stahlblech,* 1. Auflage, Düsseldorf **2003**.

How to cite this article: Babutzka M, Müller T, Mietz J, Burkert A. Investigation of the influence of iron-containing abrasives on the corrosion behaviour of the aluminium alloy AlSi1.2Mg0.4. *Materials and Corrosion*. 2020;1–13. https://doi.org/10.1002/maco.202011657